

Short Seeking Control with Minimum Jerk Trajectories for Dual Actuator Hard Disk Drive Systems

Jiagen Ding+, Federico Marcassa++ and Masayoshi Tomizuka+

+Department of Mechanical Engineering

+University of California at Berkeley, Berkeley, CA 94720-1740

++Department of Information Engineering

++University of Padova, Via Gradenigo 6/b-35131 Padova, Italy

jdging@newton.Berkeley.edu, marcassa@dei.unipd.it ,and tomizuka@me.Berkeley.edu

Abstract—This paper is concerned with short seeking control for hard disk drives with a dual actuation servo system consisting of a coarse actuator (voice coil motor, VCM) and a fine actuator (piezoelectric actuator, PZT). Short seeking refers to moving the recording head over a few tracks. The primary elements in short seeking control are the feedback controller, the feedforward controller and the reference input. These elements must be determined for each of the coarse and fine actuators. The unique feature of the proposed short seeking control scheme is on the use of two minimum jerk trajectories as reference inputs: one with a seek time typical for VCM and the other with a shorter seek time. The first one is used as the reference input for VCM and the difference between the two is used as the reference input for PZT, which makes the second faster trajectory set the actual seek time of the dual actuator system. Single rate and multi rate implementations of the proposed scheme are presented along with experimental results. The motivation for multi-rate implementation is saving of computation.

I. INTRODUCTION

The hard disk drive industry continues to strive for increased areal storage densities and reduced data access times. This necessitates performance improvements of the head positioning system in terms of fast transition from one track to another (track seeking), fast and accurate settling(track settling), and precise track following of the target track(track following). To achieve these improvements, the servo bandwidth of the head positioning system must be increased to lower the sensitivity to disturbances such as disk flutter vibrations, spindle motor run-out, windage, and external vibration.The servo bandwidth, however, is mainly limited by the mechanical resonance of the head positioning system. Dual-actuator servo systems offer one way to expand the servo bandwidth. The dual-actuator disk file system consists of two actuators: coarse and fine actuators. The coarse actuator is of low bandwidth but its stroke is large; the voice coil motor (VCM) is the most popular coarse actuator. The fine actuator is of high bandwidth but its stroke is small; the piezoelectric transducer(PZT) is a popular fine actuator. Many research groups have proposed and manufactured dual actuator prototypes. Research efforts

have also been devoted to the design of a simple and high performance dual-actuator servo system [2], [3], [4], [6].

The short seeking control is to move the Read/Write head across a few tracks to the target track. This problem may be formulated as a trajectory tracking control problem. A good overall control structure for reference trajectory tracking is the two-degree-of-freedom control structure[5]. In [5], the two-degree-of-freedom control structure was applied to the single actuator(only VCM available) seeking control. Short-span track seeking control has been proposed for a dual-actuator system in [9]. In [9], the two-degree-of-freedom control structure was adopted for a dual actuator system. The minimum jerk trajectory was utilized as the reference input in the track seeking control of single actuator disk drives in [10]. Numasato and Tomizuka utilized the minimum jerk trajectories in track seeking/settling control of dual actuator disk drives [11]. In order to ensure a smooth settling, the minimum jerk trajectory was re-designed in real time to match the states of the VCM at a certain time ahead the recording head reaches the target track.

This paper presents a short track seeking scheme for dual actuator hard disk drive systems based on minimum jerk trajectories and its single-rate and multi-rate implementations along with experimental data. The motivation for multi-rate implementation is saving of computation [12].

The remainder of this paper is organized as follows. Section II presents the structure of the dual-actuator system. Section III discusses the short seeking control design of the dual-actuator system. Section IV presents the multirate implementation of the short seeking control. Section V demonstrates a design example with experimental results. Concluding remarks are given in section VI.

II. DUAL-ACTUATOR SERVOSYSTEMS

Figure 1 shows the schematic of a hard disk drive system. It mainly consists of disks, voice coil motor(VCM), arm and Read/Write(R/W) head. In disk drive operation, a motor spins the disk as fast as 10,000 rpm and the voice coil motor(VCM) drives the arm and controls the position of

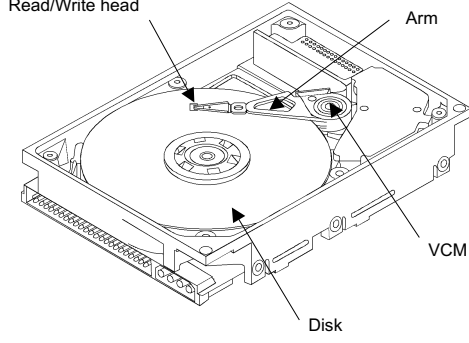


Fig. 1. Schematic Diagram of Hard Disk Drive

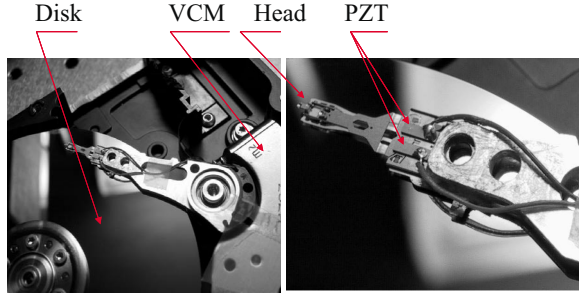


Fig. 2. Dual Actuator Servosystems

the suspension system that holds the R/W head. In this paper, we consider a dual actuator system consisting of a VCM as a coarse actuator and a PZT as a fine actuator (Fig. 2). The VCM is a conventional actuator used for commercial hard disk drive systems. The fine actuator is an active suspension, which finely moves the R/W head laterally. The fine actuator is located between the head suspension and the base plate, which is moved by VCM. A slider is attached to the tip of the suspension. The advantage of this moving suspension type actuator is that it does not require substantial modifications to the shape of the head suspension assembly. The fine actuator has two piezoelectric elements which are in parallel. The two piezoelectric elements are oppositely polarized so that one expands and the other contracts when the same voltage potential is applied to them. This results in rotation of the load beam and off track motion of a slider. Typical piezoelectric actuators attain a stroke displacement of about $1 \mu m$.

III. SHORT SEEKING CONTROL FOR DUAL ACTUATOR HDD

A. Overall Structure of Dual Actuator HDD Servo System during Short Seeking Mode

Figure 3 shows the overall structure of HDD servo system during short seeking control. It consists of the track following or regulation controller, the feedforward controller and the reference trajectory generator for each of the two actuators, VCM and PZT. In the figure, $P_{VCM}(z)$ and $P_{PZT}(z)$

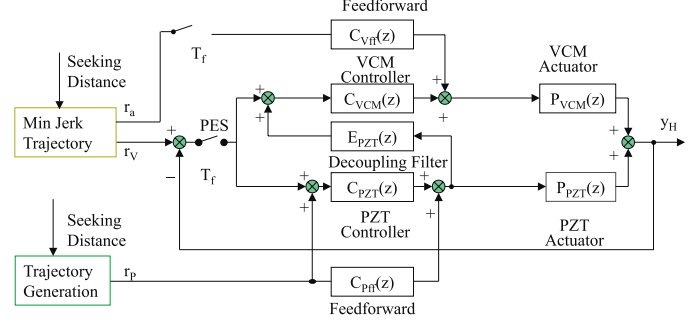


Fig. 3. Block Diagram of RTRD Dual Actuator Short Seeking Control

represent the dynamics of VCM and PZT, respectively. The feedback controllers for VCM and PZT are represented by $C_{VCM}(z)$ and $C_{PZT}(z)$, and the feedforward controller by $C_{Vff}(z)$ and $C_{Pff}(z)$. $E_{PZT}(z)$ is called the decoupling filter.

(1)The overall structure during seeking is a two-degree-of-freedom structure. As shown in the figure, both the VCM and PZT actuators receive inputs from the feedback controller and feedforward controller.

(2)In the regulation loop, the VCM and PZT paths would be parallel if the decoupling filter were zero. In this case, both the VCM controller(C_{VCM}) and the PZT controller(C_{PZT}) in the feedback loop respond to the position error signal(PES), which introduces dynamic coupling between the two actuators. If the decoupling filter closely approximates the dynamics of the PZT actuator, the output of the decoupling filter fed back to the VCM controller with a positive sign will cancel the output of the PZT actuator fed back to the VCM controller via the PES feedback signal. The cancellation implies that the VCM controller does not see the PZT loop, and in this sense the VCM loop is decoupled from the PZT loop. For this reason, $E_{PZT}(z)$ is called the decoupling filter.

(3)If the VCM feedback loop is decoupled from the PZT feedback loop, the VCM actuator output tracks the VCM reference trajectories(r_V and r_a) and the PZT actuator output tracks the PZT reference trajectory(r_P). The head position (y_H) is just the sum of the two actuator outputs. Thus, the feedforward controller design and the reference trajectory generation are also decoupled.

1) *VCM Controller Design:* To guarantee the stability of the dual-actuator system even in the case that the PZT actuator is not activated, the VCM feedback loop should be stable by itself. In the first step, the VCM controller $C_{VCM}(z)$ is designed so that the VCM feedback loop has basic performance and appropriate stability.

In the design of the feedback controller for the VCM actuator, the sensitivity of the VCM $S_{VCM}(z)$ is used as the performance index and the gain and phase margins of the VCM actuator open loop transfer function $L_{VCM}(z)$

are used for stability evaluation.

$$S_{VCM}(z) = \frac{1}{1 + C_{VCM}(z)P_{VCM}(z)} \quad (1)$$

$$L_{VCM}(z) = C_{VCM}(z)P_{VCM}(z) \quad (2)$$

In the decoupled control structure, if the PZT actuator is not switched on, the VCM actuator output y_V is related to the VCM position reference signal r_V via:

$$y_V = \frac{C_{Vff}(z)P_{VCM}(z) + C_{VCM}(z)P_{VCM}(z)}{1 + C_{VCM}(z)P_{VCM}(z)} r_V \quad (3)$$

where it has been assumed that the input to the feedforward controller $C_{Vff}(z)$ is the position reference signal(r_V).

If $C_{Vff}(z)P_{VCM}(z) \approx 1$, then $y_V \approx r_V$. In the seeking controller design, the VCM actuator model is approximately a double integrator around the specified bandwidth, so that the feedforward signal for the VCM actuator may be the acceleration reference signal, i.e. the second derivative of r_V , instead of r_V [14]. Thus, by letting the second derivative of r_V be the input to the feedforward controller, $C_{Vff}(z)$ may be reduced to a constant, i.e. the mass of the VCM actuator.

2) *PZT Controller Design*: In this step, the PZT controller $C_{PZT}(z)$ and a decoupling filter $E_{PZT}(z)$ are designed in order to achieve superior performance of the dual actuator system. The decoupling filter $E_{PZT}(z)$ is an open loop estimator of the PZT actuator output. Let the PZT loop sensitivity function be:

$$S_{PZT}(z) = \frac{1}{1 + C_{PZT}(z)P_{PZT}(z)} \quad (4)$$

If $E_{PZT}(z) = P_{PZT}(z)$, the total loop sensitivity function can be written as:

$$S_D(z) = S_{VCM}(z)S_{PZT}(z) \quad (5)$$

The total sensitivity function is the product of the VCM loop sensitivity function and the PZT loop sensitivity function. The performance index for PZT feedback controller design is the overall loop sensitivity function $S_D(z)$. Since the two actuators are decoupled, the design is reduced to shape the PZT loop sensitivity function to ensure that the total sensitivity function $S_D(z)$ satisfies the performance requirement. The gain and phase margins of the overall open loop transfer function are used as the stability measures.

Other indexes that should be considered in the PZT feedback controller design are the relative gain and phase between the equivalent VCM path and the PZT path[13].

If the VCM and PZT feedback loops are decoupled, the VCM actuator feedforward controller is $C_{Vff}(z) \approx P_{VCM}^{-1}(z)$ and the PZT actuator feedforward controller is $C_{Pff}(z) \approx P_{PZT}^{-1}(z)$, then the position outputs y_V and y_P due to VCM and PZT reference inputs r_V and r_P are respectively:

$$y_V \approx r_V, \quad y_P \approx r_P \quad (6)$$

The overall R/W head position y_H is the sum of y_V and y_P . Because of Eq. 6, the VCM and PZT actuator reference signals should be designed such that their sum is the desired reference.

B. Reference Trajectory Generation

The short seeking control objectives are achieved by computing the reference signals from time 0 to the expected seeking completion instants for the VCM and PZT actuators. The VCM actuator trajectory is generated by minimizing the jerk[11] during the transition and the PZT actuator trajectory is introduced for further shortening the seeking time.

The minimum jerk VCM trajectory $r_V(t)$ with zero initial conditions is generated by minimizing the objective function:

$$\int_0^{T_V} \left(\frac{d^3 r_V(t)}{dt^3} \right)^2 dt \quad (7)$$

subject to

$$r_V(T_V) = r_f, \quad \dot{r}_V(T_V) = 0, \quad \ddot{r}_V(T_V) = 0 \quad (8)$$

where T_V is the seeking target time for VCM actuator.

Solving this minimization problem by the Lagrange multiplier method, the position and acceleration trajectory signals are:

$$r_V(t) = \left[6\left(\frac{t}{T_V}\right)^5 - 15\left(\frac{t}{T_V}\right)^4 + 10\left(\frac{t}{T_V}\right)^3 \right] r_f \quad (9)$$

$$\ddot{r}_V(t) = \frac{1}{(T_V)^2} \left[120\left(\frac{t}{T_V}\right)^3 - 180\left(\frac{t}{T_V}\right)^2 + 60\left(\frac{t}{T_V}\right) \right] r_f \quad (10)$$

Rewrite the minimum jerk position reference signal as

$$r_V(t) = F_r(t, T_V) r_f \quad (11)$$

where $F_r(t, T_V)$ is given by

$$F_r(t, T_V) = 6\left(\frac{t}{T_V}\right)^5 - 15\left(\frac{t}{T_V}\right)^4 + 10\left(\frac{t}{T_V}\right)^3 \quad (12)$$

and may be computed offline.

When there is no PZT reference trajectory(zero reference for PZT), the R/W head will follow the VCM reference trajectory $r_V(t)$ and arrive at the target track at time T_V . If the PZT trajectory $r_P(t)$ is introduced, the R/W head will follow the trajectory $r_V(t) + r_P(t)$, the head trajectory $r_H(t)$. If this head trajectory $r_H(t)$ (Eq.13) is also a minimum jerk trajectory generated for the same final states as for $r_V(t)$ but with a shorter seeking time T_H , the R/W head will follow this minimum jerk head trajectory $r_H(t)$ and arrive at the target track at time T_H , which is sooner than T_V .

$$r_H(t) = F_r(t, T_H) r_f \quad (13)$$

where $F_r(t, T_H)$ is similarly defined as $F_r(t, T_V)$. The PZT reference trajectory is obtained by subtracting $r_V(t)$ from $r_H(t)$

$$\begin{aligned} r_P(t) &= r_H(t) - r_V(t) \\ &= (F_r(t, T_H) - F_r(t, T_V))r_f \end{aligned} \quad (14)$$

Since $r_H(t)$ and $r_V(t)$ are both minimum jerk trajectories and are smooth, the PZT reference trajectory will also be smooth. This determination of $r_P(t)$ makes sense because PZT has a higher bandwidth than VCM. It is noted that $r_P(t)$ will be zero when $T_H=T_V$. Thus, the PZT reference trajectory $r_P(t)$ may remain within the PZT saturation limit by adjusting T_H and T_V .

IV. MULTIRATE IMPLEMENTATION OF SHORT SEEKING CONTROL

The short seeking control scheme in the previous section may be implemented as single rate control or multi-rate control. In this section, we present the multirate implementation of the dual actuator short seeking control to achieve computational saving[12]. Figure 4 shows the block diagram of the multirate implementation of the dual actuator seeking control. In Fig. 4, the VCM feedback controller (C_{VCM}), the VCM feedforward controller(C_{Vff}) and the decoupling filter(E_{PZT}) are implemented at slow sampling rate($\frac{1}{mT_f}$). The D block and I block are the decimator and the repetition interpolator respectively. The slow rate controllers $C_{VCM}(z^m)$, $C_{Vff}(z^m)$ and $E_{PZT}(z^m)$ can be obtained from the fast rate controllers $C_{VCM}(z)$, $C_{Vff}(z)$ and $E_{PZT}(z)$ through the three step procedure in[12].

It is noted that the input to VCM actuator(u_{VCM}) is updated every mT_f seconds and no computation is performed at sampling instants, $(nm + i)T_f$ with $n = 0, 1, 2, \dots$ and $i = 1, 2, \dots, m - 1$, which results in computational saving. Notice that this computational saving is not uniform since the amount of computation at sampling instants $(nmT_f, n=0,1,2,\dots)$ is the same as the fast rate implementation. Interlacing implementation of the slow rate controllers makes computation saving uniform at all fast rate sampling instants[12]. For example, assume that the multirate ratio m is selected so that the VCM fast rate controller $C_{VCM}(z)$ may be naturally decomposed to m blocks: i.e.

$$C_{VCM}(z) = C_{VCM1}(z) + C_{VCM2}(z) + \dots + C_{VCMm}(z) \quad (15)$$

where $n_c = n_{c1} + n_{c2} + \dots + n_{cm}$, n_c is the order of $C_{VCM}(z)$ and n_{ci} is the order of $C_{VCMi}(z)$ ($i=1,2, \dots,m$). Obviously

$$n_{max} = \max_i(n_{ci}) < n_c \quad (16)$$

Applying the three step procedure[12], the controller for the slow sampling rate is

$$C_{VCM}(z^m) = C_{VCM1}(z^m) + C_{VCM2}(z^m) + \dots + C_{VCMm}(z^m) \quad (17)$$

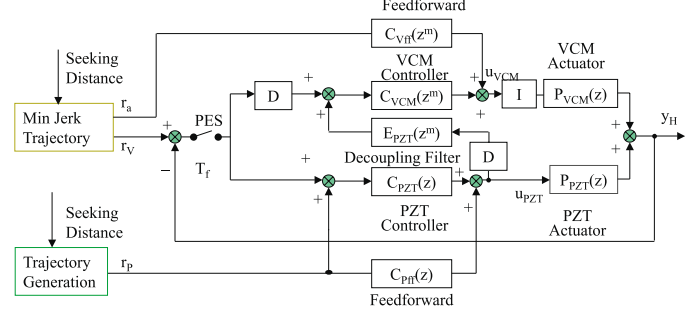


Fig. 4. Block Diagram of Multirate RTRD Dual Actuator Short Seeking Control

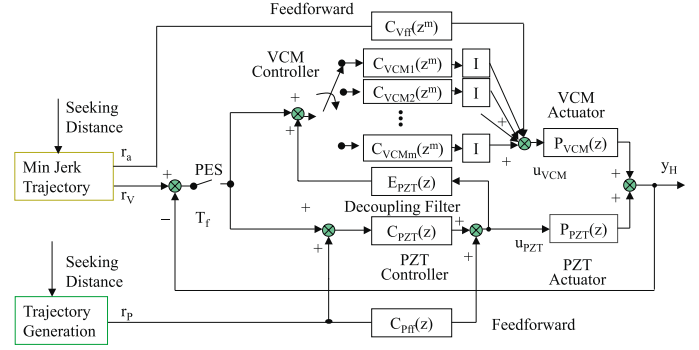


Fig. 5. Slow Rate Implementation of $C_{VCM}(z)$ with Interlacing

Instead of updating $C_{VCMi}(z^m)$ ($i=1,2,\dots,m$) all at the same sampling instances, $C_{VCMi}(z^m)$ may be updated one block at a time at fast sampling instances: i.e. update C_{VCMi} at $k = mj + i - 1$ ($j = 0, 1, 2, \dots$). This is an interlacing operation, and the controller implementation diagram becomes as shown in Fig.5. Note that m slow blocks are updated sequentially one at a time at each fast sampling instance and that the decoupling filter is updated at each fast sampling instance. In this implementation, the amount of computation required at each fast sampling instance is equivalent to or less than that of implementing an n_{max} -th order digital controller, and computational saving is more uniform by distributing computation among each fast sampling point. Thus, the computational saving for the whole short seeking becomes more uniform if the multirate interlacing implementation is also applied to the slow rate controller $C_{Vff}(z^m)$.

V. DESIGN EXAMPLE

A. Short Seeking Controller Design

In this section, we present a design example of short seeking control of a dual actuator hard disk drive. The design specification is to achieve an $1.0kHz$ or higher bandwidth, an about 40° phase margin and a $4dB$ or larger gain margin. The spindle speed is $7200rpm$. The experimental setup for a dual actuator disk drive is depicted in Fig.6. It includes a conventional actuator voice coil

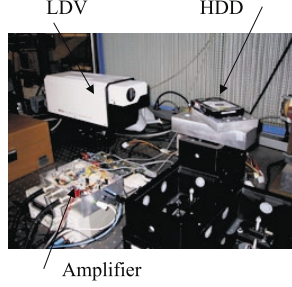


Fig. 6. Dual Actuator Setup

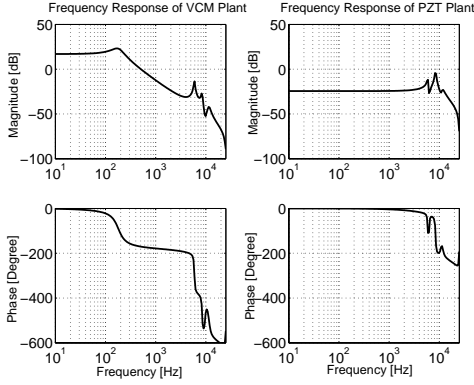


Fig. 7. Frequency Response of Plants

motor, a Hutchinson PZT based micro-actuator, a digital signal processor(TI TMS230C67X DSP), and a laser Doppler vibrometer(LDV) for measuring the position error. All the digital controllers are implemented on the DSP using C code. The fast sampling rate is $50kHz$ and the slow sampling rate is $\frac{50}{3}kHz$.

Figure 7 shows the transfer functions of VCM and PZT actuator models. Notice that the gain plot of the VCM frequency response exhibits resonant peaks at 5.8, 8.2 and $11.5kHz$. The phase of VCM frequency response is close to -180° around $600Hz$ due to the effect of double integration. The PZT frequency response is flat with phase lag close to zero at low frequencies and increasing at high frequencies due to the resonant frequency at $8.2kHz$.

The fast rate VCM feedback controller is:

$$C_{VCM}(z) = 2.6927 \frac{(z - 0.9822)(z - 0.9652)(z - 0.9589)}{(z - 1)(z - 0.9363)(z - 0.8397)} \quad (18)$$

and it includes an integrator and a second order phase compensator. This controller may be decomposed to three first-order blocks for slow rate implementation with interlacing. The slow rate VCM feedback controller is:

$$C_{VCM_{lr}}(z^3) = 2.3901 \frac{(z^3 - 0.9476)(z^3 - 0.8922)(z^3 - 0.8816)}{(z^3 - 1)(z^3 - 0.820)(z^3 - 0.5855)} \quad (19)$$

Recall that the input to the VCM feedforward controller is the second derivative of r_V and the VCM feedforward

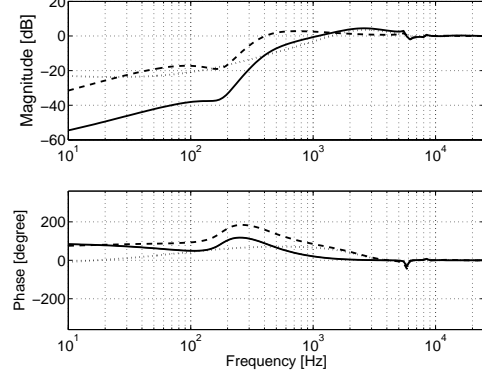


Fig. 8. Sensitivity Functions

controller is a constant gain, which is the mass of the VCM actuator:

$$C_{Vff}(z) = 8.9876e - 8 \quad (20)$$

The PZT feedback controller is given by:

$$C_{PZT}(z) = 1.0799 \frac{(z - 1)(z - 0.3217)}{(z - 0.9991)(z - 0.9883)} \times \frac{(z^2 - 1.075z + 0.9914)(z^2 - 0.8545z + 1.242)}{(z - 0.1613)^2(z - 0.4754)(z - 0.149)} \quad (21)$$

This PZT controller has a zero at 1 so that the frequency response gain of PZT path is low at low frequencies but is relatively high from $100Hz$ to $1kHz$. Notice that this PZT controller also includes 2 notch filters for notching out resonant peaks. Since the frequency response of the PZT actuator is flat at low frequencies, the PZT estimator is approximated by a constant with one step delay(Eq.22) and the PZT feedforward controller is a constant, which is proportional to the inverse of the DC gain of the PZT actuator (Eq.23).

$$E_{PZT}(z) = 0.06z^{-1} \quad (22)$$

$$C_{Pff}(z) = 13.333 \quad (23)$$

Table I summarizes the design results.

TABLE I
DESIGN RESULTS

	VCM loop	PZT loop	Total loop
Gain Margin(dB)	22.4	13.5	10.5
Phase Margin($^\circ$)	47.3	62.9	48.2
Cross Over Frequency(Hz)	500	1350	14100

Figure 8 shows three sensitivity functions: the solid line corresponds to the dual actuator sensitivity, the dot line to the PZT loop sensitivity and the dash line to the single VCM loop sensitivity. The dual actuation achieves better disturbance rejection compared to the VCM actuator only.

Figure 9 shows the fast rate $125nm$ track seek experimental results, which corresponds to one track seek for a $200KTPI$ disk drive. The implementation of the controller

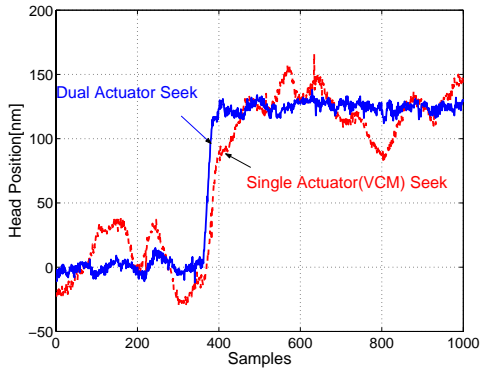


Fig. 9. 125nm seeking waveform Comparison

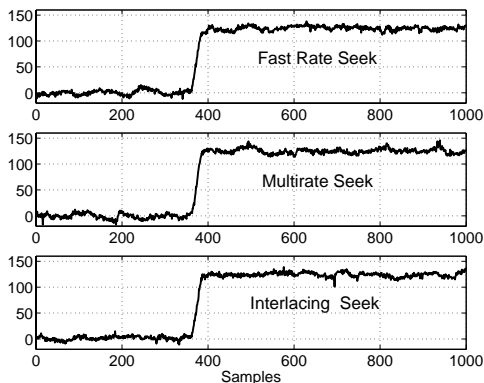


Fig. 10. 125nm seeking waveforms

is single rate. The solid line is the head position response for fast rate dual actuator seeking and the dashed line is the head position response for single actuator seeking. In the experiment, the track seek started at the sampling point 350 for both dual actuator and single actuator seeking control with $T_V = 40\text{samples}$ and $T_H = 25\text{samples}$. Notice that dual actuator seeking achieves fast settling and small steady error. Figure 10 compares the single rate implementation of the short track seeking controller to the multi-rate implementations with and without interlacing. Notice that there is no significant difference between multirate and single fast rate implementation. The amount of computation in terms of clock cycles for different implementation is summarized in Table II. The VCM multirate implementation achieves 46% computational saving on the average while the multirate with interlacing saves computation about 36%. Thus, the multirate scheme saves a significant amount of computation without noticeable performance degradation.

TABLE II
COMPUTATION OF DIFFERENT IMPLEMENTATIONS

	Fast Rate	Multirate	Interlacing
PZT (Cycles)	255	251	251
VCM (Cycles)	253	135	160

VI. CONCLUSION

In this paper, a short track seeking control scheme for dual actuator disk drive systems was presented. The unique aspect of the scheme was the use of two minimum jerk trajectories: one of the two trajectories was used as the reference signal for the VCM actuator, while the other was used to set the reference signal for the PZT actuator. This allowed the R/W head under dual actuation to reach and settle on the target track faster than single actuation by VCM. Multi-rate implementation of the short track seeking controller achieved a significant saving of computation without serious performance degradation. Experimental results verified the effectiveness of the proposed approach.

VII. ACKNOWLEDGEMENTS

This research was conducted at the Computer Mechanics Laboratory(CML) in the Department of Mechanical Engineering, University of California at Berkeley.

REFERENCES

- [1] Grochowski and R. Hoyt, "Future trends in hard disk drives", *IEEE Transactions on Magnetics*, vol.32, pp.1850-1854, May 1996.
- [2] S. K. Aggarwal, D. A. Horsley, R. Horowitz, and A. P. Pisano, "Micro-actuators for High Density Disk Drives", in *Proceedings of the American Control Conference*, Albuquerque, New Mexico, pp.3979-3984, June, 1997.
- [3] S. Koganezawa, Y. Uematsu and T. Yamada, "Dual-Stage Actuator System for Magnetic Disk Drives Using a Shear Mode Piezoelectric Microactuator", *IEEE Transactions on Magnetics*, vol.35, pp.988-992, March 1999.
- [4] D. A. Horsley, N. Wongkomet, R. Horowitz, and A. P. Pisano, "Precision Positioning Using a Microfabricated Electrostatic Actuator", *IEEE Transactions on Magnetics*, vol.35, pp.993-999, March 1999.
- [5] L. Yi, "Two Degree of Freedom control for Disk Drive Servo Systems", PhD Thesis, University of California at Berkeley, Fall 2000
- [6] D. A. Horsley, D. Hernandez, R. Horowitz, A. K. Packard and A. P. Pisano, "Closed-Loop Control of a Microfabricated Actuator for Dual Stage Hard Disk Drive Servo Systems", in *Proceedings of the American Control Conference*, Philadelphia, PA, June, 1998.
- [7] D.T. Phan "The Design and Modeling of Multirate Digital Control System for Disk Drive Applications", *Proceedings of the 1993 Asia-Pacific Workshop on Advances in motion control*, Singapore, pp.189-205, July 1993.
- [8] T. Hara "Multi-rate Controller for Hard Disk Drive with Redesign of State Estimator", *Proceedings of the American Conference*, Philadelphia, Pennsylvania, June 1998.
- [9] M. Kobayashi and R. Horowitz, "Track Seek Control for Hard Disk Drive Dual-Stage Servo Systems", in *Transaction on Magnetics*, Vol. 37, No. 2, March 2001.
- [10] Y. Mizoshita, S. Hasegawa, and K. Takaishi, "Vibration minimized access control for disk drives, *IEEE Transaction on Magnetics*, vol. 32, pp.17931798, May 1996.
- [11] H. Numasato and M. Tomizuka, "Settling Control and Performance of Dual-Actuator System for Hard Disk Drives", in *Proceedings of the American Control Conference*, Arlington, VA, pp.2779-2785, June 2001.
- [12] J. Ding, F. Marcassa, S. Wu and M. Tomizuka, "Multirate Control for Computational Saving", Computer Mechanics Lab Research Reports (13), 2003.
- [13] J. Ding, M. Tomizuka and H. Numasato, "Design and Robustness Analysis of Dual Stage Servo System", in *Proceedings of the American Control Conference*, Chicago, IL, pp.2605-2609, June 2000.
- [14] J. Ding, "Digital Control of Dual Actuator Hard Disk Drives", Ph.D. thesis, University of California at Berkeley, Fall 2003.